Biochemical and Biophysical Research Communications 461 (2015) 136–141

Contents lists available at ScienceDirect

Biochemical and Biophysical Research Communications

journal homepage: www.elsevier.com/locate/ybbrc

Myelin basic protein is a glial microtubule-associated protein – Characterization of binding domains, kinetics of polymerization, and regulation by phosphorylation and a lipidic environment

Agata Zienowicz, Vladimir V. Bamm, Kenrick A. Vassall, George Harauz*

Department of Molecular and Cellular Biology, University of Guelph, 50 Stone Road East, Guelph, Ontario N1G 2W1, Canada

ARTICLE INFO

Article history:
Received 24 March 2015
Available online 7 April 2015

Keywords:
Myelin basic protein
Intrinsically-disordered proteins
Microtubule-associated proteins
Phosphorylation
Oligodendrocyte cytoskeleton
Dodecylphosphocholine (DPC)

ABSTRACT

The 18.5-kDa splice isoform of myelin basic protein (MBP) predominates in the adult brain, adhering the cytoplasmic leaflets of the oligodendrocyte membrane together, but also assembling the cytoskeleton at leading edges of membrane processes. Here, we characterized MBP's role as a microtubule-assembly protein (MAP). Using light scattering and sedimentation assays we found that pseudo-phosphorylation of Ser54 (murine 18.5-kDa sequence) significantly enhanced the rate but not the final degree of polymerization. This residue lies within a short KPGSG motif identical to one in tau, a ubiquitous MAP important in neuronal microtubule assembly. Using polypeptide constructs, each comprising one of three major amphipathic α-helical molecular recognition fragments of 18.5-kDa MBP, we identified the N-terminal α1-peptide as sufficient to cause microtubule polymerization, the rate of which was significantly enhanced in the presence of dodecylphosphocholine (DPC) micelles to mimic a lipidic environment.

1. Introduction

Myelin basic protein (MBP) is essential for the formation of myelin of the central nervous system of higher vertebrates [1–3]. The predominant 18.5-kDa classic splice isoform holds the cytoplasmic leaflets of the oligodendrocyte membrane in close apposition, but also assembles microfilaments and microtubules at the leading edges of membrane processes being extended to form the sheath [3,4]. The protein is intrinsically disordered and interacts with various partners via short molecular recognition fragments (MoRFs) that undergo local disorder-to-order transitions, with modulation by myriad post-translational modifications [4–6]. The 18.5-kDa MBP has also been identified as a microtubule-associated protein (MAP) in bovine brain and in cultured oligodendrocytes by co-immuno-precipitation and co-localization [7–12]. Phosphorylation of MBP at unknown sites has been reported to strengthen the protein's ability to polymerise and bundle microtubules *in vitro* [13], and to increase its interaction with microtubules in oligodendrocytes [14]. However, phosphorylation specifically at Thr94 and Thr97 (of the bovine isoform, corresponding to Thr92 and Thr95 in the murine 18.5-kDa sequence numbering, Fig. 1A) had little effect on its ability to polymerise and bundle microtubules, but decreased its ability to bind them to the membrane surface *in vitro* [15]. Charge reduction of the protein by pseudo-deimination at 6 sites throughout the sequence also decreased its ability to tether microtubules to membranes [15]. Furthermore, MBP and these modified forms were able to bind microtubules and microfilaments to each other [15]. Thus, many studies support the idea that, at the tips of the extending oligodendrocyte membrane processes that will form the compact regions of myelin, 18.5-kDa MBP may also tether the cytoskeleton to the membrane, bundle microfilaments and microtubules and bind them to each other, and help regulate process extension, retraction, and axonal ensheathment [3,4]. The effect of seryl-specific phosphorylation of MBP by protein kinase C has not yet been investigated, but there is a linear motif found in both MBP and in tau (a primarily neuronal MAP) that comprises a phosphorylated Ser54 (murine 18.5-kDa MBP sequence numbering, Fig. 1A) [16]. Our goals here were to map the segments of MBP that interact with tubulin, and to investigate the modulatory roles of site-specific seryl pseudo-phosphorylation.

* Corresponding author. Fax: +1 519 837 1802.
E-mail address: gharauz@uoguelph.ca (G. Harauz).

http://dx.doi.org/10.1016/j.bbrc.2015.03.181
0006-291X/

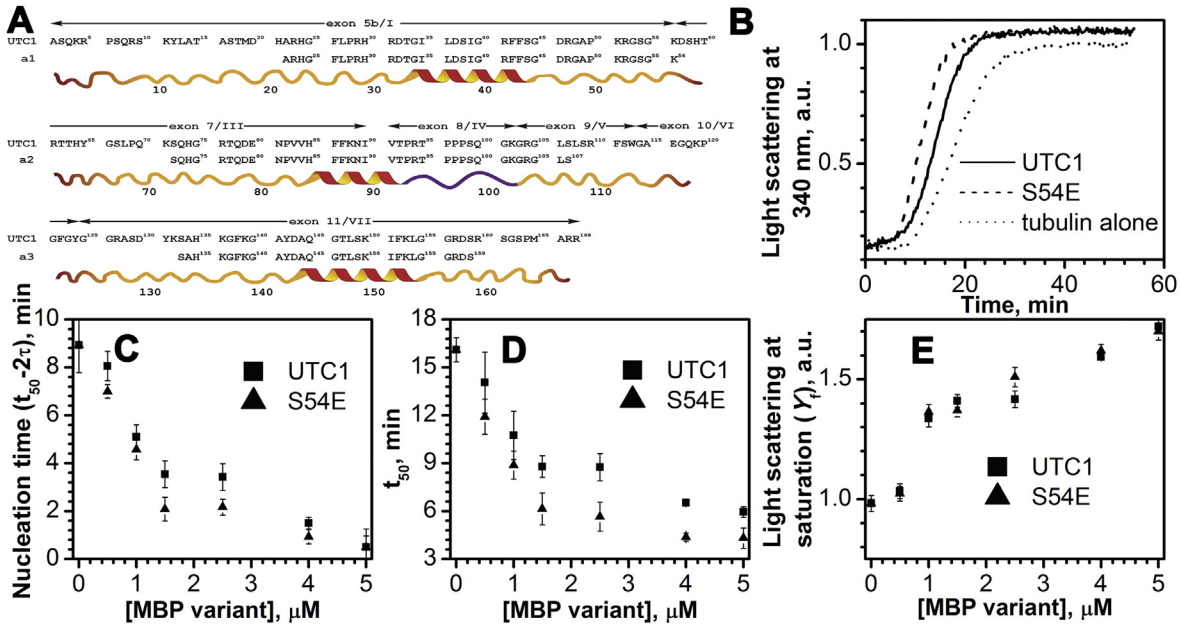

Fig. 1. (A) Sequences of murine 18.5-kDa MBP variants (168 amino acids). The 1st row indicates the exons (*golli* numbering in Arabic/Sanskrit numerals, classic numbering in Roman numerals). The 2nd row indicates the "untagged" (no C-terminal LEH_6 purification tag, as in our previous studies) C1 (unmodified) charge component. The 3rd row shows the α-peptides comprising the main membrane-anchoring amphipathic α-helices. The 4th row represents the main secondary structure elements of 18.5-kDa MBP in a myelin environment. This figure has been adapted from Ref. [4]. (B) Time-based light scattering profiles of microtubule assembly (10 μM tubulin) in the presence of unmodified and pseudo-phosphorylated 18.5-kDa MBP variants (0.5 μM each). This figure is representative of at least three replicates. The following parameters are plotted as a function of MBP charge variant concentration: (C) length of nucleation phase (or lag-time, $t_{50} - 2\tau$), (D) t_{50}, and (E) light scattering at saturation (Y_f). Data are presented as means ± standard deviations calculated from analysis performed by fitting individual kinetic curves (Figure S2) using Eq. (1). Each kinetic curve was replicated at least three times and analyzed individually.

2. Materials and methods

2.1. Purification of proteins and peptides

Tubulin was obtained from fresh bovine brain using established methods [17]. The unmodified 18.5-kDa recombinant murine MBP isoform (C1 component of MBP), UTC1, was expressed in *E. coli* BL21-CodonPlus(DE3)-RP cells (Stratagene, La Jolla, CA), in untagged ("UT") form, *i.e.*, without any purification tags, and purified as described [18]. The pseudo-phosphorylated variant of UTC1 with a single S54E substitution was generated by site-directed mutagenesis [19]. The α1-, α2-, and α3-segments of murine 18.5-kDa MBP encoding residues (A22-K56), (S72-S107), and (S133-S159), respectively, were cloned into the Champion™ pET SUMO (small ubiquitin modifier) Expression System (Invitrogen Life Technologies, Burlington, ON) and purified as described with a final HPLC step [20]. Standard curves for each α-peptide were created using HPLC to ensure that consistent and accurate protein concentrations were used in all assays (Figure S1).

2.2. Kinetics of microtubule assembly induced by MBP variants

Light scattering was used to probe microtubule polymerization [13]. All components required for the assay, except tubulin and GTP, were premixed. Because of its lability, tubulin was thawed and added as the last reagent. Stocks of MBP full-length variants and MBP-α-peptides of known concentration were made by resuspending known weights of lyophilized proteins in MilliQ water. Concentrations were routinely re-verified spectrophotometrically, or by injecting 10-μL samples into the HPLC and extrapolating concentration from the calibration curves (Figure S1).

Time-based light scattering profiles of microtubule assembly were collected at different MBP (or α-peptide):tubulin molar ratios ranging from 0.05 to 0.5 (or 0.75–90), in the final reaction volume of 60 μL in GPEM buffer (80 mM PIPES-KOH, 1 mM EGTA, 1 mM $MgCl_2$, 1 mM GTP, pH 6.9). First, concentrations of each MBP full-length charge variant or α-peptide in the range of 0–5 μM and 0–900 μM, respectively, were prepared in PEM buffer (80 mM PIPES-KOH, 1 mM EGTA, 1 mM $MgCl_2$, pH 6.9). Then, pre-frozen stocks of bovine tubulin were thawed quickly in room temperature water and placed immediately on ice. Pre-made GTP stocks (10 mM GTP, pH 7.6 with NaOH) were added to the tubulin stock and allowed to incubate on ice for 5 min. Tubulin/GTP stocks were then added to each pre-heated (to 37° C) working reaction mixture to a final concentration of 10 μM tubulin and 1 mM GTP, and immediately read (at 37° C) using a microplate reader (Polarstar Omega, BMG Laboratory Technologies, Offenburg, Germany). In comparative experiments, the detergent dodecylphosphocholine (DPC, Avanti Polar Lipids, Alabaster, AL) was added to a final working concentration of 1.2 mM (above its critical micellar concentration of 1.0 mM) prior to the addition of the tubulin/GTP mixture. Measurements were done in time-based absorbance mode, assuming that any change in light intensity passing through the sample (*i.e.*, at 180°) was due to light scattering and not absorbance. A total of 250 measurements were taken at an interval of 13 s. At least three replicates at each molar ratio were measured and analyzed independently. Data were analyzed using ORIGIN software (version 8.0, OriginLab Corporation, Northhampton, MA).

2.3. Nucleation-dependent polymerization (NDP) analysis

The light scattering curves were fitted to the equation:

$$Y_t = (s_i t + Y_i) + \left[(s_f t + Y_f) - (s_i t + Y_i)\right] \Big/ \left[1 + \exp(-(t - t_{50})/\tau)\right] \quad (1)$$

where Y_t is the light scattering signal in arbitrary units (AU) obtained at time t, Y_f is the y-intercept of the final linear region that describes saturation, Y_i is the y-intercept of the initial linear region

that describes lag-time (t_{lag}, nucleation phase), s_i is the initial slope of the curve (*i.e.*, during the nucleation phase), s_f is the final slope of the curve (*i.e.*, during the saturation phase), t_{50} is the time to reach 50% maximal light scattering, and τ is a characteristic time constant (Figure S2). Variables t_{50}, Y_f, and τ ($t_{lag} = t_{50}$-2τ) were obtained as fitted parameters from the Origin program and were used to assess changes in polymerization kinetics quantitatively. All three replicates for each condition were analyzed independently and plotted as means and standard deviations.

2.4. Polymerization and sedimentation assays of microtubule assembly induced by MBP-α1-peptide with/without DPC

The critical concentrations of tubulin in the presence and absence of 7.5 μM MBP-α1-peptide and 1.2 mM DPC were determined by monitoring the change in light scattering at 340 nm of solutions containing varying concentrations of tubulin. The light scattering at saturation was determined by NDP analysis and was plotted *versus* the tubulin concentration, with the *x*-intercepts yielding the critical tubulin concentration (C_c) [21].

To determine the apparent binding constant K_d and the stoichiometry (n) between MBP-α1-peptide and microtubule assemblies in the presence and absence of DPC, we employed a sedimentation assay as we did previously to investigate binding between MBP-α-peptides and actin assemblies [22], and calculated from the equation:

$$\frac{[\alpha 1_B]}{[Tubulin_t]} = \frac{n \cdot [\alpha 1_f]}{K_d + [\alpha 1_f]}, \quad (2)$$

where $[\alpha 1_B]$ is the concentration of α1-peptide bound to tubulin (*i.e.*, α1-peptide in the pellet), $[Tubulin_t]$ is the total tubulin concentration (*i.e.*, total tubulin concentration = 10 μM), n is the stoichiometry of the interaction (*i.e.*, the ratio of α1-peptide bound to every αβ-tubulin heterodimer), $[\alpha 1_f]$ is the amount of free α1-peptide (*i.e.*, α1-peptide in the supernatant), and K_d is the apparent dissociation constant. The values of $[\alpha 1_f]$, $[\alpha 1_B]$, and $[Tubulin_t]$ were measured experimentally. The values of n and K_d were determined by plotting $[\alpha 1_B]/[Tubulin_t]$ *versus* $[\alpha 1_f]$, and fitting data points to the above equation using Origin software. Each point is represented as the mean of data obtained from two independent experiments.

3. Results

3.1. Parameters of tubulin polymerization by 18.5-kDa MBP charge variants

Tubulin polymerization in the presence of varying concentrations of two 18.5-kDa MBP charge variants was monitored by change in light scattering at 340 nm (Fig. 1B): the unmodified form, termed UTC1, and a variant pseudo-phosphorylated at one site, termed S54E (Fig. 1A). The seryl pseudo-phosphorylation site is part of a motif that is found in both tau and classic MBP isoforms, and that is phosphorylated in both proteins [3,16]. Both charge variants showed a concentration-dependent ability to alter length of nucleation phase (also referred to as lag phase), but MBP-S54E had the shorter lag phase (Fig. 1C), as well as a decreased time to reach 50% maximal light scattering (t_{50}) (Fig. 1D). Both variants had comparable degrees of light scattering at saturation (Fig. 1E).

3.2. The N-terminal MBP-α1-peptide can induce tubulin polymerization alone and DPC enhances this effect

Tubulin polymerization was evaluated in the presence of three MBP-α-peptides (referred to as α1-, α2-, and α3-peptides and corresponding to A22-K56, S72-S107 and S133-S159, respectively), and in the presence and absence of 1.2 mM DPC as a membrane mimetic. Traces of light scattering at 340 nm were collected and analyzed using non-linear curve fitting to Eq. (1) (NDP method). Only the α1-peptide enhanced tubulin polymerization kinetics beyond GPEM buffer alone, more than would be expected by the net charge difference compared to the other two peptides (Figure S3). The α1-peptide was able to increase light scattering measured at saturation in a concentration-dependent manner – 700 μM being required in the absence of DPC, but only 250 μM in its presence – to reach plateau (Fig. 2A). Therefore, although the α1-peptide can cause the assembly of a similar mass of polymer, much lower concentrations of it are needed to do so in the presence of DPC.

The α1-peptide showed a concentration-dependent ability to alter nucleation time in both the presence and absence of DPC (Fig. 2C). In the absence of DPC, high concentrations of α1-peptide caused a moderate, but significant, decrease in the nucleation time of polymerization. However, α1-peptide concentrations as high as 500 μM were unable to abolish the nucleation phase completely. In the presence of DPC, the α1-peptide dramatically shortened nucleation time and was able to abolish nucleation time completely at concentrations as low as approximately 12.5 μM. The α1-peptide caused a concentration-dependent decrease in t_{50} in both the absence and presence of DPC (Fig. 2D). In the presence of DPC, α1-peptide at only 30 μM was required to abolish t_{50} completely, compared to 700 μM in its absence.

The apparent binding constant (K_d) and the stoichiometry of binding (n) between the MBP-α1-peptide and tubulin, in the presence and absence of DPC, were determined using a sedimentation assay coupled with HPLC quantification (Fig. 2B). In the presence of DPC, K_d was 30.4 ± 10.3 μM, and n was 18.3 ± 2.2. In the absence of DPC, K_d was 467.6 ± 25.7 μM when n was fixed to 18. Therefore, in the presence of DPC, the stoichiometry of binding is not altered, but the value of K_d decreases drastically.

To determine the critical concentration, light scattering by tubulin solutions of varying concentrations was measured at 340 nm (Fig. 3A, B). Light scattering at saturation was determined using the NDP method and was plotted *versus* the tubulin concentration (Fig. 3C). Applying a linear regression to these data allowed the critical tubulin concentration (C_c) to be determined from the *x*-intercepts. The C_c was four times smaller in the presence of 7.5 μM α1-peptide (C_c = 0.24 ± 0.03 μM and 0.27 ± 0.06 μM, without or with DPC, respectively) than in its absence (0.93 ± 0.03 μM with DPC, and 0.97 ± 0.03 μM without DPC). These concentrations are significantly lower compared to the previously published C_c of tubulin when polymerization was induced by glycerol [23], and are comparable to the one (0.69 μM) previously reported for full-length MBP [13].

4. Discussion

The classic isoforms of MBP are expressed primarily in the later stages of oligodendrocyte differentiation (in contrast to the earlier developmental golli-isoforms that arise from the same gene complex), and range from 14 to 21.5 kDa in nominal molecular mass [3]. In mature compact myelin, 18.5-kDa MBP keeps the cytoplasmic leaflets of the oligodendrocyte membrane in tight apposition to form the major dense line. But even mature myelin is structurally heterogeneous [24] and undergoes constant remodeling [25]. The

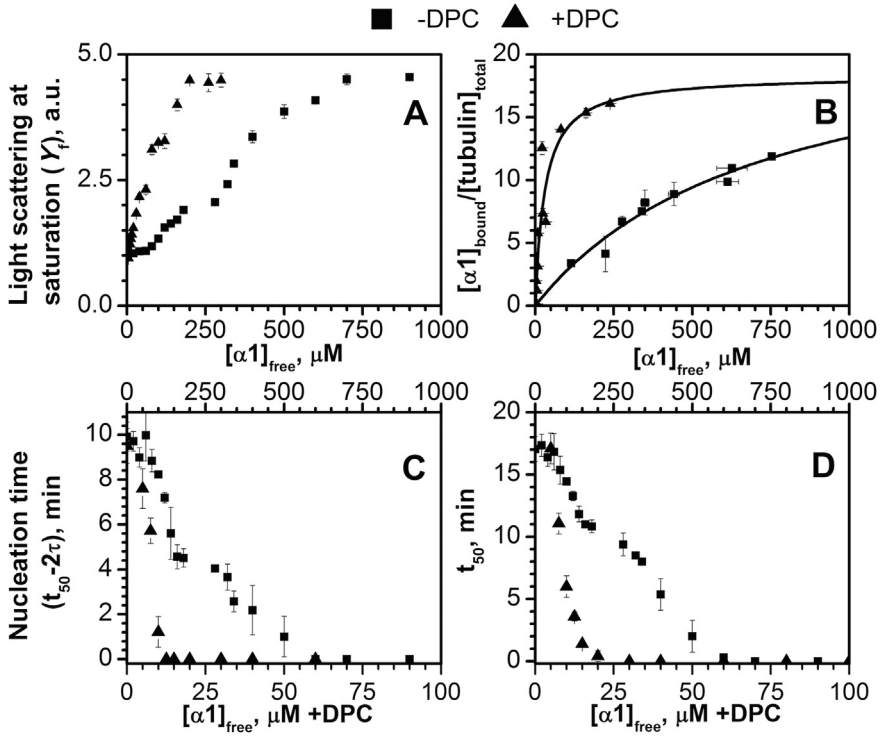

Fig. 2. The MBP-α1-peptide, especially with DPC, affects microtubule assembly kinetics. The microtubule assembly kinetics (Figure S2, panels C and D) were analyzed using NDP method. Data are presented as means ± standard deviations calculated from analysis performed by fitting individual kinetic curves to Eq. (1). Each kinetic curve was replicated at least three times and analyzed individually. The following parameters are plotted as a function of α1-peptide concentration in the presence and absence of 1.2 mM DPC: (A) light scattering at saturation (Y_f), (C) length of nucleation phase (or lag-time, $t_{50} - 2\tau$), and (D) t_{50}. (B) Determining the apparent dissociation constant (K_d) and stoichiometry of binding (n) of α1-peptide and tubulin in the presence and absence of DPC using a sedimentation assay. Data are presented as means ± standard deviations of three replicates, and binding parameters (K_d and n) were extrapolated by fitting the data to a one-site binding model (Eq. (2)).

dynamic molecular barcode of post-translational modifications of 18.5-kDa MBP (tabulated in Refs. [3,6]) serves to target it to different microdomains of myelin and to modulate its interactions with membranes and with other proteins, with which it acts as a hub in a variety of networks [3,4,6,26–29].

We have extended here our first detailed *in vitro* study of MBP-induced microtubule polymerization and bundling [13]. There, the different 14-kDa to 21.5-kDa murine MBP splice isoforms were produced in recombinant form by over-expression in *E. coli*, yielding a compositionally pure protein product, and we concluded that the classic exons III and IV were most likely to comprise the tubulin-interaction sites (Fig. 1A). We have since created a new recombinant MBP construct lacking a hexa-histidine tag, which could potentially interfere with quantitative measurements of assembly kinetics [18]. We used primarily a light scattering polymerization assay in which kinetic traces show three major phases of nucleation, elongation, and saturation. To extract additional parameters, we used a nucleation-dependent polymerization analysis to reflect that tubulin assembly involves intermediate aggregates, not just nuclei [30]. This approach has been used in kinetic analyses of amyloidogenesis by monellin and insulin [31,32].

Previously, we also compared 18.5-kDa MBP charge components C1–C6 (purified from bovine brain) which vary primarily in degree of phosphorylation, and observed that this modification strengthened MBP's ability to assemble tubulin, the opposite of its effect on MBP-induced actin assembly [13,33]. Since MBP isolated from brain is compositionally heterogeneous because of the many PTMs, recombinant proteins also represent a *tabula rasa* to evaluate site-

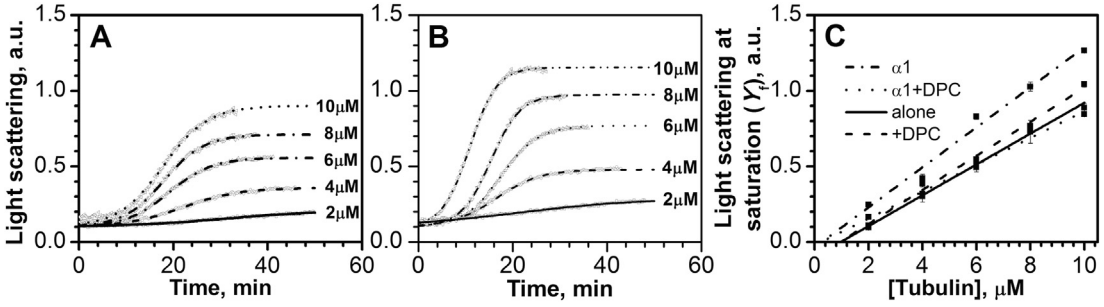

Fig. 3. The critical concentration of tubulin decreases 4-fold in the presence of α1-peptide and is unaltered by the presence of DPC. An example of the light scattering traces observed for increasing concentrations of tubulin polymerized by 7.5 μM α1-peptide in the absence (A) or presence of DPC (B). (C) The critical concentrations of tubulin in the presence and absence of both α1-peptide and DPC are extrapolated from linear regression to $y = 0$. Light scattering at saturation was determined by the NDP method. Averages of three replicates are displayed as points, and standard deviations are reported as error bars.

specific modifications such as (pseudo-)phosphorylation. Here, we focused on residue S54 to test the hypothesis that the $K^{51}P^{52}G^{53}S^{54}G^{55}$ motif (identical to the one found in the MAP tau) is involved directly in the association between the two proteins [16]. We constructed a pseudo-phosphorylated S54E variant and demonstrated that this single site-specific modification resulted in a significant decrease in microtubule nucleation time, supporting the hypothesis. This observation is also congruent with the report that phosphorylation of MBP in oligodendrocytes stimulated by phorbol esters (which activate protein kinase C pathways) increased its interactions with microtubules [14].

We have also used recombinantly-expressed MBP fragments comprising amphipathic α-helical segments involved in molecular recognition [20], and have localized the tubulin interaction site more definitively to comprise the first amphipathic α-helical segment of MBP, *viz*., the α1-peptide. This region of the protein has previously been shown to interact with membranes [34], to be sufficient to polymerize actin, and to be another calcium-activated calmodulin target [20]. We thus have a further example of "moonlighting", whereby MBP, like other intrinsically-disordered proteins, has "MoRFs" that can interact specifically with different targets, either in competition or in different contexts [5,35]. The rate of microtubule assembly by the α1-peptide was significantly enhanced in a lipidic environment (DPC micelles), an observation that supports our proposition that, at the tips of the extending membrane processes to form the compact regions of myelin, 18.5-kDa MBP may also tether the cytoskeleton to the membrane, bundle microfilaments and microtubules together and to each other, and help regulate process extension and retraction and axonal ensheathment [3,4,15].

The "*Tao*" of MBP as a MAP begs comparison with the protein tau, the quintessential MAP of neuronal cells [36]. Like MBP, tau is intrinsically-disordered and its phosphorylation status affects its function: phosphorylated tau can still promote tubulin assembly under some conditions but hyper-phosphorylated tau has a diminished ability to do so. In a recent commentary entitled "why brains need tau", Amos suggests that the various isoforms are required to contribute to the dynamic growth of microtubule arrays in axonal process extensions interactively with other cellular components [37]. We know that MBP is needed to hold compact myelin together, but "why do brains need MBP to assemble microtubules"? Even though tau has also been detected in oligodendrocytes and has been co-localized with MBP [38–40], it may be that classic MBP isoforms afford the extra dimension of membrane tethering, and that their sheer abundance overshadows any effects of tau at the cell periphery [15].

Conflict of interest

The authors have no conflicts of interest to declare.

Acknowledgments

This work was supported by the Natural Sciences and Engineering Research Council of Canada (RG121541 to G.H.), and by the Canada Research Chairs Program (to G.H.). K.A.V. was the recipient of a Postdoctoral Fellowship from the Multiple Sclerosis Society of Canada. We are grateful to Dr. Joan Boggs for helpful comments on the work and on manuscript, and to Mr. Brian MacDougall for access to bovine brain.

Appendix A. Supplementary data

Supplementary data related to this article can be found at http://dx.doi.org/10.1016/j.bbrc.2015.03.181.

References

[1] S. Nawaz, J. Schweitzer, O. Jahn, H.B. Werner, Molecular evolution of myelin basic protein, an abundant structural myelin component, Glia 61 (2013) 1364–1377.
[2] M. Bakhti, S. Aggarwal, M. Simons, Myelin architecture: zippering membranes tightly together, Cell. Mol. Life Sci. 71 (2013) 1265–1277.
[3] G. Harauz, J.M. Boggs, Myelin management by the 18.5-kDa and 21.5-kDa classic myelin basic protein isoforms, J. Neurochem. 125 (2013) 334–361.
[4] G. Harauz, V. Ladizhansky, J.M. Boggs, Structural polymorphism and multifunctionality of myelin basic protein, Biochemistry 48 (2009) 8094–8104.
[5] D.S. Libich, M.A.M. Ahmed, L. Zhong, V.V. Bamm, V. Ladizhansky, G. Harauz, Fuzzy complexes of myelin basic protein: NMR spectroscopic investigations of a polymorphic organizational linker of the central nervous system, Biochem. Cell. Biol. 88 (2010) 143–155 (Special Issue on Protein Folding: Principles and Diseases).
[6] G. Harauz, D.S. Libich, E. Polverini, K.A. Vassall, The classic protein of myelin – conserved structural motifs and the dynamic molecular barcode involved in membrane adhesion, protein-protein interactions, and pathogenesis in multiple sclerosis, in: B.M. Dunn (Ed.), Advances in Protein and Peptide Science (e-book, Bentham Science Publishers, 2013, pp. 1–53. http://benthamscience.com/ebooks/9781608054879/index.htm.
[7] M. Taketomi, N. Kinoshita, K. Kimura, M. Kitada, T. Noda, H. Asou, T. Nakamura, C. Ide, Nogo-A expression in mature oligodendrocytes of rat spinal cord in association with specific molecules, Neurosci. Lett. 332 (2002) 37–40.
[8] F. Kozielski, T. Riaz, S. Debonis, C.J. Koehler, M. Kroening, I. Panse, M. Strozynski, I.M. Donaldson, B. Thiede, Proteome analysis of microtubule-associated proteins and their interacting partners from mammalian brain, Amino Acids 41 (2011) 363–385.
[9] M.R. Galiano, A. Andrieux, J.C. Deloulme, C. Bosc, A. Schweitzer, D. Job, M.E. Hallak, Myelin basic protein functions as a microtubule stabilizing protein in differentiated oligodendrocytes, J. Neurosci. Res. 84 (2006) 534–541.
[10] M.R. Galiano, C. Lopez Sambrooks, M.E. Hallak, Insights into the interaction of myelin basic protein with microtubules, in: J.M. Boggs (Ed.), Myelin Basic Protein, Intrinsically Disordered Proteins, Nova Science Publishers, New York, 2008, pp. 129–147.
[11] G.S.T. Smith, L. Homchaudhuri, J.M. Boggs, G. Harauz, Classic 18.5- and 21.5-kDa myelin basic protein isoforms associate with cytoskeletal and SH3-domain proteins in the immortalized N19-oligodendroglial cell line stimulated by phorbol ester and IGF-1, Neurochem. Res. 37 (2012) 1277–1295.
[12] J.M. Boggs, L. Homchaudhuri, G. Ranagaraj, Y. Liu, G.S. Smith, G. Harauz, Interaction of myelin basic protein with cytoskeletal and signaling proteins in cultured primary oligodendrocytes and N19 oligodendroglial cells, BMC Res. Notes 7 (2014) 387, 391-387-14.
[13] C.M.D. Hill, D.S. Libich, G. Harauz, Assembly of tubulin by classic myelin basic protein isoforms and regulation by post-translational modification, Biochemistry 44 (2005) 16672–16683.
[14] M.R. Galiano, M.E. Hallak, Phosphorylation of MBP increased its interaction with microtubules in oligodendrocytes, neuroscience 2008, in: 2008 Neuroscience Meeting Proceedings, Society for Neuroscience, Washington, DC, 2008.
[15] J.M. Boggs, G. Rangaraj, Y.M. Heng, Y. Liu, G. Harauz, Myelin basic protein binds microtubules to a membrane surface and to actin filaments *in vitro*: effect of phosphorylation and deimination, Biochim. Biophys. Acta (Biomembranes) 1808 (2011) 761–773.
[16] J. Karthigasan, H. Inouye, D.A. Kirschner, Implications of the sequence similarities between tau and myelin basic protein, Med. Hypotheses 45 (1995) 235–240.
[17] M. Castoldi, A.V. Popov, Purification of brain tubulin through two cycles of polymerization-depolymerization in a high-molarity buffer, Protein Expr. Purif. 32 (2003) 83–88.
[18] G.S.T. Smith, L. Chen, V.V. Bamm, J.R. Dutcher, G. Harauz, The interaction of zinc with membrane-associated 18.5 kDa myelin basic protein: an attenuated total reflectance-Fourier transform infrared spectroscopic study, Amino Acids 39 (2010) 739–750.
[19] G.S.T. Smith, M. De Avila, P.M. Paez, V. Spreuer, M.K.B. Wills, N. Jones, J.M. Boggs, G. Harauz, Proline substitutions and threonine pseudophosphorylation of the SH3 ligand of 18.5-kDa myelin basic protein decrease its affinity for the Fyn-SH3 domain and alter process development and protein localization in oligodendrocytes, J. Neurosci. Res. 90 (2012) 28–47.
[20] V.V. Bamm, M. De Avila, G.S.T. Smith, M.A. Ahmed, G. Harauz, Structured functional domains of myelin basic protein: cross talk between actin polymerization and Ca(2+)-dependent calmodulin interaction, Biophys. J. 101 (2011) 1248–1256.
[21] K.A. Johnson, G.G. Borisy, Kinetic analysis of microtubule self-assembly *in vitro*, J. Mol. Biol. 117 (1977) 1–31.
[22] V.V. Bamm, M.A. Ahmed, G. Harauz, Interaction of myelin basic protein with actin in the presence of dodecylphosphocholine micelles, Biochemistry 49 (2010) 6903–6915.
[23] J.C. Lee, S.N. Timasheff, *In vitro* reconstitution of calf brain microtubules: effects of solution variables, Biochemistry 16 (1977) 1754–1764.

[24] G.S. Tomassy, D.R. Berger, H.H. Chen, N. Kasthuri, K.J. Hayworth, A. Vercelli, H.S. Seung, J.W. Lichtman, P. Arlotta, Distinct profiles of myelin distribution along single axons of pyramidal neurons in the neocortex, Science 344 (2014) 319–324.
[25] K.M. Young, K. Psachoulia, R.B. Tripathi, S.J. Dunn, L. Cossell, D. Attwell, K. Tohyama, W.D. Richardson, Oligodendrocyte dynamics in the healthy adult CNS: evidence for myelin remodeling, Neuron 77 (2013) 873–885.
[26] J.M. Boggs, P.M. Yip, G. Rangaraj, E. Jo, Effect of posttranslational modifications to myelin basic protein on its ability to aggregate acidic lipid vesicles, Biochemistry 36 (1997) 5065–5071.
[27] G. Harauz, A.A. Musse, A tale of two citrullines - structural and functional aspects of myelin basic protein deimination in health and disease, Neurochem. Res. 32 (2007) 137–158.
[28] L.S. DeBruin, G. Harauz, White matter rafting - membrane microdomains in myelin, Neurochem. Res. 32 (2007) 213–228.
[29] K.A. Vassall, K. Bessonov, M. De Avila, E. Polverini, G. Harauz, The effects of threonine phosphorylation on the stability and dynamics of the central molecular switch region of 18.5-kDa myelin basic protein, PLoS One 8 (2013) e68175, 1-19.
[30] H. Flyvbjerg, E. Jobs, S. Leibler, Kinetics of self-assembling microtubules: an “inverse problem” in biochemistry, Proc. Natl. Acad. Sci. U. S. A. 93 (1996) 5975–5979.
[31] A.T. Sabareesan, J.B. Udgaonkar, Amyloid fibril formation by the chain B subunit of monellin occurs by a nucleation-dependent polymerization mechanism, Biochemistry 53 (2014) 1206–1217.
[32] L. Nielsen, R. Khurana, A. Coats, S. Frokjaer, J. Brange, S. Vyas, V.N. Uversky, A.L. Fink, Effect of environmental factors on the kinetics of insulin fibril formation: elucidation of the molecular mechanism, Biochemistry 40 (2001) 6036–6046.
[33] C.M.D. Hill, G. Harauz, Charge effects modulate actin assembly by classic myelin basic protein isoforms, Biochem. Biophys. Res. Commun. 329 (2005) 362–369.
[34] I.R. Bates, J.M. Boggs, J.B. Feix, G. Harauz, Membrane-anchoring and charge effects in the interaction of myelin basic protein with lipid bilayers studied by site-directed spin labeling, J. Biol. Chem. 278 (2003) 29041–29047.
[35] P. Tompa, C. Szasz, L. Buday, Structural disorder throws new light on moonlighting, Trends Biochem. Sci. 30 (2005) 484–489.
[36] M. Morris, S. Maeda, K. Vossel, L. Mucke, The many faces of tau, Neuron 70 (2011) 410–426.
[37] L.A. Amos, Why do brains need tau (MAPT)? FEBS J. 281 (2014) iv–v.
[38] P. LoPresti, S. Szuchet, S.C. Papasozomenos, R.P. Zinkowski, L.I. Binder, Functional implications for the microtubule-associated protein tau: localization in oligodendrocytes, Proc. Natl. Acad. Sci. U. S. A. 92 (1995) 10369–10373.
[39] C. Klein, E.M. Kramer, A.M. Cardine, B. Schraven, R. Brandt, J. Trotter, Process outgrowth of oligodendrocytes is promoted by interaction of fyn kinase with the cytoskeletal protein tau, J. Neurosci. 22 (2002) 698–707.
[40] V. Seiberlich, N.G. Bauer, L. Schwarz, C. Ffrench-Constant, O. Goldbaum, C. Richter-Landsberg, Downregulation of the microtubule associated protein Tau impairs process outgrowth and myelin basic protein mRNA transport in oligodendrocytes, Glia (2015), http://dx.doi.org/10.1002/glia.22832 in press online.